

Typhoon effect on Kuroshio and Green Island wake: a modelling study

T.-W. Hsu et al.

This discussion paper is/has been under review for the journal Ocean Science (OS).
Please refer to the corresponding final paper in OS if available.

Typhoon effect on Kuroshio and Green Island wake: a modelling study

T.-W. Hsu^{1,2}, M.-H. Chou², T.-H. Hou², and S.-J. Liang³

¹Research Center for Ocean Energy and Strategies, National Taiwan Ocean University, Keelung, Taiwan

²Department of Hydraulic and Ocean Engineering, National Cheng-Kung University, Tainan, Taiwan

³Department of Marine Environmental Informatics, National Taiwan Ocean University, Keelung, Taiwan

Received: 15 October 2015 – Accepted: 4 December 2015 – Published: 21 December 2015

Correspondence to: S.-J. Liang (sjliang@ntou.edu.tw)

Published by Copernicus Publications on behalf of the European Geosciences Union.

Title Page

Abstract Introduction

Conclusions References

Tables Figures

◀ ▶

◀ ▶

Back Close

Full Screen / Esc

Printer-friendly Version

Interactive Discussion



Abstract

Green Island located in the typhoon active eastern Taiwan coastal water is the potential Kuroshio power plant site. In this study, a high resolution (250–2250 m) shallow-water equations (SWEs) model is used to investigate the effect of typhoon on the hydrodynamics of Kuroshio and Green Island wake. Two wind induced flows, typhoon Soulik and Holland's wind field model, are studied. Simulation results of the typhoon Soulik indicate that salient characteristics of Kuroshio and downstream island wake seems less affected by the typhoon Soulik because typhoon Soulik is 250 km away Green Island and the wind speed near Green Island is small. Moreover, Kuroshio currents increase when flow is in the same direction as the counterclockwise rotation of typhoon, and vice versa. This finding is in favorable agreements with the TOROS observed data.

The SWEs model, forced by the Kuroshio and Holland's wind field model, successfully reproduces the downstream recirculation and meandering vortex street. Numerical results unveil that the slow moving typhoon has a more significant impact on the Kuroshio and downstream Green Island wake than the fast moving typhoon does. Due to the counterclockwise rotation of typhoon, Kuroshio currents increase (decrease) in the right (left) of the moving typhoon's track. This rightward bias phenomenon is evident, especially when typhoon moves in the same direction as the Kuroshio mainstream.

1 Introduction

According to Zdravkovich (2003) flow past a bluff obstacle with the Reynolds number $Re = u_\infty L / \nu_t$ in the range of 50 and 800, a well-organized downstream wake occurs, where u_∞ is the characteristic flow velocity, L the characteristic length, and ν_t the eddy viscosity of fluid. Flow becomes periodic with detachment of the free shear layer, and consequently alternate shedding of vortices. The periodic phenomenon is referred to as

OSD

12, 3199–3233, 2015

Typhoon effect on Kuroshio and Green Island wake: a modelling study

T.-W. Hsu et al.

Title Page

Abstract

Introduction

Conclusions

References

Tables

Figures



Back

Close

Full Screen / Esc

Printer-friendly Version

Interactive Discussion



stresses are given as

$$\tau_x^s = \rho_{\text{air}} C_{D_s} \sqrt{W_{10x}^2 + W_{10y}^2} W_{10x} \quad (5)$$

$$\tau_y^s = \rho_{\text{air}} C_{D_s} \sqrt{W_{10x}^2 + W_{10y}^2} W_{10y} \quad (6)$$

Where W_{10x} and W_{10y} are the x and y component of W_{10} , C_{D_s} is the coefficient of surface stresses (Zhang and Sannasiraj, 2008).

2.2 Space–Time Least-Squares Finite-Element Method

We use the two-dimensional SWEs to illustrate the Space–Time Least-Squares Finite-Element Method (STLSFEM). The two-dimension SWEs read

$$\begin{aligned} \frac{\partial \eta}{\partial t} + u \frac{\partial (H + \eta)}{\partial x} + (H + \eta) \frac{\partial u}{\partial x} + v \frac{\partial (H + \eta)}{\partial y} + (H + \eta) \frac{\partial v}{\partial y} &= 0 \\ \frac{\partial u}{\partial t} + u \frac{\partial u}{\partial x} + v \frac{\partial u}{\partial y} &= S_x \\ \frac{\partial v}{\partial t} + u \frac{\partial v}{\partial x} + v \frac{\partial v}{\partial y} &= S_y \end{aligned} \quad (7)$$

where $S_x = \frac{\tau_x^s - \tau_x^b}{\rho h} - g \frac{\partial Z_b}{\partial x}$, $S_y = \frac{\tau_y^s - \tau_y^b}{\rho h} - g \frac{\partial Z_b}{\partial y}$. The Newton method is applied to linearize the nonlinear terms in Eq. (7), and the resulting equations are

$$\begin{aligned} \frac{\partial \eta}{\partial t} + H \frac{\partial u}{\partial x} + u \frac{\partial H}{\partial x} + \frac{\partial}{\partial x} (\tilde{\eta} u + \eta \tilde{u} - \tilde{\eta} \tilde{u}) + H \frac{\partial v}{\partial y} + v \frac{\partial H}{\partial y} + \frac{\partial}{\partial y} (\tilde{\eta} v + \eta \tilde{v} - \tilde{\eta} \tilde{v}) &= 0 \\ \frac{\partial u}{\partial t} + \left(\tilde{u} \frac{\partial u}{\partial x} + u \frac{\partial \tilde{u}}{\partial x} - \tilde{u} \frac{\partial \tilde{u}}{\partial x} \right) + \left(\tilde{v} \frac{\partial u}{\partial y} + v \frac{\partial \tilde{u}}{\partial y} - \tilde{v} \frac{\partial \tilde{u}}{\partial y} \right) &= \tilde{S}_x \\ \frac{\partial v}{\partial t} + \left(\tilde{u} \frac{\partial v}{\partial x} + u \frac{\partial \tilde{v}}{\partial x} - \tilde{u} \frac{\partial \tilde{v}}{\partial x} \right) + \left(\tilde{v} \frac{\partial v}{\partial y} + v \frac{\partial \tilde{v}}{\partial y} - \tilde{v} \frac{\partial \tilde{v}}{\partial y} \right) &= \tilde{S}_y \end{aligned} \quad (8)$$

where the symbol “ \sim ” denotes the value from the previous iteration or time step. In the STLSFEM, the unknowns $\tilde{u} = \{\tilde{\eta}, u, v\}^T$ are approximated by the polynomial interpolations

$$\begin{Bmatrix} \eta(x, y, t) \\ u(x, y, t) \\ v(x, y, t) \end{Bmatrix} = \begin{bmatrix} M(x, y) N(t) \\ M(x, y) N(t) \\ M(x, y) N(t) \end{bmatrix} \begin{Bmatrix} \eta \\ u \\ v \end{Bmatrix} \quad (9)$$

5 where $M(x)$ and $N(t)$ are the space and time interpolation functions, respectively. Substituting the approximations Eq. (9) into Eq. (10), the residuals can be written as

$$\begin{aligned} & \begin{Bmatrix} R_\eta^e \\ R_u^e \\ R_v^e \end{Bmatrix} = \\ & \begin{bmatrix} MN'_2 & (HM_x + H_x M) N_2 & (HM_y + H_y M) N_2 \\ 0 & MN'_2 + \{\tilde{u}_x M_x + \tilde{u}_x M + \tilde{v}_y M_y\} N_2 & \tilde{u}_y MN_2 \\ 0 & \tilde{v}_x MN_2 & MN'_2 + \{\tilde{u}_x M_x + \tilde{v}_y M_y + \tilde{v}_y M\} N_2 \end{bmatrix} \begin{Bmatrix} \eta \\ u \\ v \end{Bmatrix}^{n+1} \\ & + \begin{bmatrix} MN'_1 & (HM_x + H_x M) N_1 & (HM_y + H_y M) N_1 \\ 0 & MN'_1 + \{\tilde{u}_x M_x + \tilde{u}_x M + \tilde{v}_y M_y\} N_1 & \tilde{u}_y MN_1 \\ 0 & \tilde{v}_x MN_1 & MN'_1 + \{\tilde{u}_x M_x + \tilde{v}_y M_y + \tilde{v}_y M\} N_1 \end{bmatrix} \begin{Bmatrix} \eta \\ u \\ v \end{Bmatrix}^n \\ & + \begin{Bmatrix} \tilde{S}_\eta \\ \tilde{S}_u \\ \tilde{S}_v \end{Bmatrix} \quad (10) \end{aligned}$$

Note that a piecewise continuous linear interpolation function for time is used, where the subscripts 1 and 2 denote the number of spatial local nodes, and superscripts n and $n + 1$ denote the values of the space-time element at $t = t^n$ and $t = t^{n+1}$, respectively.

Typhoon effect on Kuroshio and Green Island wake: a modelling study

T.-W. Hsu et al.

Title Page	
Abstract	Introduction
Conclusions	References
Tables	Figures
◀	▶
◀	▶
Back	Close
Full Screen / Esc	
Printer-friendly Version	
Interactive Discussion	



scales of downstream Green Island wake due to passing of the Kuroshio has been numerically studied (Liang et al., 2013). The main difference between Liang et al. (2013) and the present study lies in the point that a constant inflow used in Liang et al. (2013) is replaced by a spatial varying inflow from HYCOM in the present study.

The SWEs model is applied to simulation the typhoon Soulik event. Typhoon Soulik hit Taiwan area during 7 to 14 July 2013. Figure 4 depicts the track of typhoon Soulik. Typhoon Soulik, developed from a tropic depression on 7 July 2013 through a tropical storm, moderate typhoon, severe typhoon, and then to decrease its strength and make landfall on Taiwan on 7 December 2013. The typhoon Soulik data with the temporal interval every 6 h are from the CWB of Taiwan, which are computed by the NFS (Non-hydrostatic Forecast System). NFS uses the structured orthogonal meshes, however, SWEs model uses the unstructured triangular meshes. Therefore, wind data needs to be interpolated into the computational nodes of the SWEs model. The IDW (inverse distance weighted interpolation; Shepard, 1962) is employed to interpolate the data from NFS into nodal points of the SWEs model. In this study, the 5 km resolution typhoon Soulik data is used. The maximum wind speed of typhoon Soulik is 51 m s^{-1} , categorized as a severe typhoon. The closest distance of typhoon to Green Island is about 250 km. The maximum wind speed of the model area is 17 m s^{-1} and the average value is smaller than 10 m s^{-1} .

Figure 5a depicts the global view of the study area, where the enclosed region near the Green Island indicates the sub-domain that will be presented in the succeeding plots of the downstream recirculation and island wakes. Figure 5b depicts the local view of the sub-domain as well as location of the cross section Q_0Q_1 and monitor point P downstream Green Island, where time series of flow quantities are presented and analyzed. Length of Q_0Q_1 is 20 km. It locates about 22 km downstream the Green Island.

Figure 6 depicts the typhoon wind field and flow streamlines as well as vectors of wind (red) and flow (blue) along cross section Q_0Q_1 at S_0 – S_4 five time instances with a 12 h of increment, shown in Fig. 5, where S_0 represents 00:00 of 12 July, S_1 12:00

Typhoon effect on Kuroshio and Green Island wake: a modelling study

T.-W. Hsu et al.

Title Page

Abstract

Introduction

Conclusions

References

Tables

Figures



Back

Close

Full Screen / Esc

Printer-friendly Version

Interactive Discussion



Typhoon effect on Kuroshio and Green Island wake: a modelling study

T.-W. Hsu et al.

Title Page

Abstract

Introduction

Conclusions

References

Tables

Figures

◀

▶

◀

▶

Back

Close

Full Screen / Esc

Printer-friendly Version

Interactive Discussion



of 12 July, S_2 00:00 of 13 July, S_3 12:00 of 13 July, and S_4 00:00 of 14 July, 2013, respectively. As can be seen, the downstream island wake is well reproduced. The flow field is affected by the typhoon, especially in the shallow water area and the lee of the islands. Interactions of Kuroshio and downstream island wake with typhoon is obvious. When typhoon approaches the study area, because of the cyclonic rotation and southward winding of typhoon, Kuroshio current decreases. At S_3 , it is the moment when the center of typhoon is closest to the Green Island. The wind starts to change its direction and to blow northward. Comparing flow vectors along cross section Q_0Q_1 at S_2 with that at S_1 and S_3 of Fig. 6, it is noticed that downstream island wake is significantly affected. Kuroshio currents increase after S_2 due to the northward winding and resumes its normal flow condition after typhoon passes far away.

Figure 7a illustrates the location of 22.84° N ($y = 150$ km) cross section, where black dots denote the position of TOROS data, and Fig. 7b and c depicts the comparison of the TOROS observed surface currents with the computed flow vectors along the 22.84° N cross section at S_0 – S_4 five time instances. Since TOROS data are the surface flow quantities, they are larger than the depth-averaged model predictions, in general. Moreover, the left one-third of the cross section (0–20 km) is right in the lee of Green Island. The meandering downstream island wake is observed in the modelling, but not present in the TOROS data, because of its coarse spatial resolution (~ 10 km). However, computed results show Kuroshio currents increase when flow is in the same direction as the counterclockwise rotation of typhoon, and vice versa. This finding is consistent with the TOROS measured datasets (Lu et al., 2014).

3.2 Effect of model typhoon on Green Island wake

Figure 8 depicts flow streamlines around the Green Island of no wind forcing in a period of vortex shedding. There are small recirculations in the lee of Green Island. Its size is about the size of the island (~ 8 km). A well-organized coherent and alternating asymmetric meandering eddies in the lee of the Green Island is reproduced, which has been observed in field measurement (Chang et al., 2013) and

satellite images (Liang et al., 2013; Zheng and Zheng, 2014). In this study, simulation using the boundary conditions based on HYCOM produces a more realistic Kuroshio flow and downstream Green Island wakes.

According to the statistical analysis of typhoons from 1911 to 2010 by the CWB of Taiwan, 83.6 % of typhoons pass the eastern Taiwan coastal waters and 13.5 % pass the western Taiwan coastal waters. Therefore, two typical tracks of typhoons, namely the SN typhoon (17 % of total) moving from southwest to northeast and the EW typhoon (67 % of total) moving from east to west, shown in Fig. 9, are chosen to investigate the effect of typhoon on the Kuroshio and Green Island wake. Two typical values of the typhoon moving speed, 2.5 m s^{-1} (9 km h^{-1}) and 5.0 m s^{-1} (18 km h^{-1}), are considered. Value of the radius of maximum wind speed $R_{mw} = 50 \text{ km}$ and pressure of typhoon center $p_c = 950 \text{ hPa}$ are used in the Holland's wind field model. The resulting maximum of W_{10} is about 47 m s^{-1} .

In order to better quantify the net influence of typhoon on Green Island wake, we subtract the flow field of SN typhoon case and EW typhoon case with no wind forcing case. The net influence of typhoon on the flow field is defined by

$$U_{\text{net}} = U_{\text{wind}} - U_{\text{no wind}} \quad (13)$$

$$V_{\text{net}} = V_{\text{wind}} - V_{\text{no wind}} \quad (14)$$

Figures 10 and 11 show the “net” u and v contours of SN typhoon at $T_0 - T_2$ three time instances as indicated in Fig. 16. It is noted that the effect of typhoon on the y component velocity are more pronounced than on the x component velocity, because the direction of moving SN typhoon and the mainstream of Kuroshio is the same, in general. Due to the counterclockwise rotation of typhoon, flow accelerates (decelerates) when it flows in the favorable (adverse) direction of wind. For example, Figs. 14 and 15 show that y component velocity increases in the right of SN typhoon's track and decreases in the left of SN typhoon's track, the so called rightward bias phenomenon. The rightward bias phenomenon of u contours is not as evident as v contours, since the

Typhoon effect on Kuroshio and Green Island wake: a modelling study

T.-W. Hsu et al.

Title Page

Abstract

Introduction

Conclusions

References

Tables

Figures

◀

▶

◀

▶

Back

Close

Full Screen / Esc

Printer-friendly Version

Interactive Discussion



northeastward Kuroshio and x component wind forcing are not in the same or opposite direction.

Comparing Fig. 10 with Fig. 11, we notice that the impact of the slow moving typhoon ($W_T = 2.5 \text{ m s}^{-1}$) is more significant than the fast moving typhoon ($W_T = 5.0 \text{ m s}^{-1}$), especially in the y component velocity when typhoon moves in favor of the Kuroshio mainstream direction. When typhoon moves slowly, it takes longer time to travel the same distance. Therefore, more momentum and energy are input to water, and water takes more time to respond to the wind forcing.

Figure 12 plots the wind field as well as wind vectors (red) and flow (blue) vectors along $\overline{Q_0Q_1}$ at T_0 – T_2 three time instances. The flow field and downstream island wake are significantly affected by the northeastward typhoon. Kuroshio currents increase as typhoon approaches and decrease as typhoon passes away.

Figures 13 and 14 plot the “net” u and v contours of EW typhoon at T_0 – T_2 three time instances indicated in Fig. 16. The rightward bias feature due to the counterclockwise rotation of typhoon is evident, especially for the slow moving typhoon and y component velocities. Comparing Figs. 10 and 11 with Figs. 13 and 14, the impact of SN typhoon on the Kuroshio and downstream Green Island wake is apparently more significant than EW typhoon. The effect of typhoon strengthens when typhoon moves in favor of the Kuroshio and weakens when typhoon moves against the Kuroshio.

Figure 15 plots the wind field as well as wind vectors (red) and flow vectors (blue) along $\overline{Q_0Q_1}$ at T_0 – T_2 three time instances of EW typhoon case. The flow field and downstream island wake are also significantly affected by the EW typhoon. Kuroshio currents decrease as typhoon approaches and increase in a short period as typhoon passes away.

Figure 16 shows a comparison of time series of u and v of the monitor point P of no wind forcing case and SN typhoon case with (a) $W_T = 2.5 \text{ m s}^{-1}$ and (b) $W_T = 5.0 \text{ m s}^{-1}$, respectively. Three vertical lines are drawn and represent the three time instances. The first time instance (T_0), represented by the red vertical dashed line, indicates the time instance when typhoon is located 50 km southwest of Green Island. The second

Typhoon effect on Kuroshio and Green Island wake: a modelling study

T.-W. Hsu et al.

Title Page

Abstract

Introduction

Conclusions

References

Tables

Figures



Back

Close

Full Screen / Esc

Printer-friendly Version

Interactive Discussion



Typhoon effect on Kuroshio and Green Island wake: a modelling study

T.-W. Hsu et al.

Title Page

Abstract

Introduction

Conclusions

References

Tables

Figures



Back

Close

Full Screen / Esc

Printer-friendly Version

Interactive Discussion



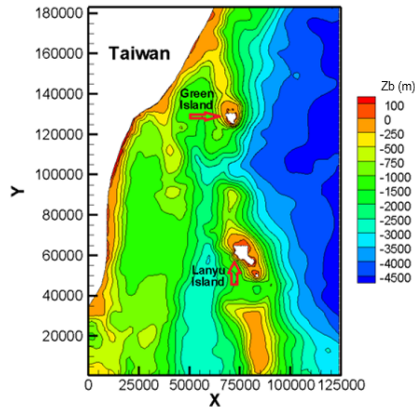
- Chen, F.: The Kuroshio Power Plant, The Kuroshio Power Plant, Springer, Singapore, Springer, 2013.
- Dong, C., McWilliams, J. C., and Shchepetkin, A. F.: Island wakes in deep water, *J. Phys. Oceanogr.*, 37, 962–981, 2007.
- 5 Gunduz, M. and Özsoy, E.: Modelling seasonal circulation and thermohaline structure of the Caspian Sea, *Ocean Sci.*, 10, 459–471, doi:10.5194/os-10-459-2014, 2014.
- Gunzburger, M. D.: *Finite Element Methods for Viscous Incompressible Flows: a Guide to Theory, Practice, and Algorithms*, Elsevier, Singapore, 2012.
- Heywood, K. J., Stevens, D. P., and Bigg, G. R.: Eddy formation behind the tropical island of Aldabra, *Deep-Sea Res. Pt. I*, 43, 555–578, 1996.
- 10 Holland, G. J., Belanger, J. I., and Fritz, A.: A revised model for radial profiles of hurricane winds, *Mon. Weather Rev.*, 138, 4393–4401, 2010.
- Hsin, Y. C., Wu, C. R., and Shaw, P. T.: Spatial and temporal variations of the Kuroshio east of Taiwan, 1982–2005: a numerical study, *J. Geophys. Res.-Oceans*, 113, C04002-1–C04002-15, doi:10.1029/2007JC004485, 2008.
- 15 Hsu, T.-W., Doong, D.-J., Hsieh, K.-J., and Liang, S.-J.: Numerical study of Monsoon effect on Green Island Wake, *J. Coastal Res.*, 31, 1141–1150, doi:10.2112/JCOASTRES-D-14-00206.1, 2015.
- Hubert, L. and Krueger, A.: Satellite pictures of mesoscale eddies, *Mon. Weather Rev.*, 90, 457–463, 1962.
- 20 Hughes, T. J. and Hulbert, G. M.: Space-time finite element methods for elastodynamics: formulations and error estimates, *Comput. Method. Appl. M.*, 66, 339–363, 1988.
- Jiang, B.-N.: *The Least-Squares Finite Element Method: Theory and Applications in Computational Fluid Dynamics and Electromagnetics*, Springer Science & Business Media, Berlin, German, 2013.
- 25 Johnson, R.: *A Modern Introduction to the Mathematical Theory of Water Waves*, Cambridge University Press, Cambridge, 1997.
- Laible, J. P. and Pinder, G. F.: Solution of the shallow water equations by least squares collocation, *Water Resour. Res.*, 29, 445–455, 1993.
- 30 Li, X., Clemente-Colón, P., Pichel, W. G., and Vachon, P. W.: Atmospheric vortex streets on a RADARSAT SAR image, *Geophys. Res. Lett.*, 27, 1655–1658, 2000.
- Liang, S.-J., and Hsu, T.-W.: Least-squares finite-element method for shallow-water equations with source terms, *Acta Mech. Sinica*, 25, 597–610, 2009.

Typhoon effect on Kuroshio and Green Island wake: a modelling study

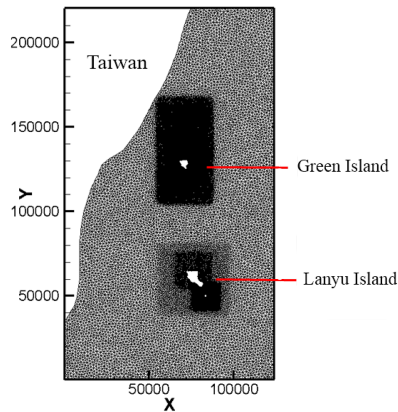
T.-W. Hsu et al.

[Title Page](#)[Abstract](#)[Introduction](#)[Conclusions](#)[References](#)[Tables](#)[Figures](#)[Back](#)[Close](#)[Full Screen / Esc](#)[Printer-friendly Version](#)[Interactive Discussion](#)

- Wolanski, E., Imberger, J., and Heron, M.: Island wakes in shallow coastal waters, *J. Geophys. Res.-Oceans*, 89, 10553–10569, 1984.
- Young, G. S. and Zawislak, J.: An observational study of vortex spacing in island wake vortex streets, *Mon. Weather Rev.*, 134, 2285–2294, 2006.
- 5 Yulistiyanto, B., Zech, Y., and Graf, W.: Flow around a cylinder: shallow-water modeling with diffusion-dispersion, *J. Hydraul. Eng.-ASCE*, 124, 419–429, 1998.
- Zdravkovich, M. M.: *Flow around Circular Cylinders, Volume 2: Applications*, Oxford University Press, Oxford, UK, 2003.
- Zhang, H. and Sannasiraj, S.: Wind wave effects on surface stress in hydrodynamic modeling, in: *The Eighth ISOPE Pacific/Asia Offshore Mechanics Symposium*, International Society of Offshore and Polar Engineers, Vancouver, Canada, November 10–14, 2008.
- 10 Zheng, Q., Lin, H., Meng, J., Hu, X., Song, Y. T., Zhang, Y., and Li, C.: Submesoscale ocean vortex trains in the Luzon Strait, *J. Geophys. Res.-Oceans*, 113, C04032-1–C04032-12, doi:10.1029/2007JC004362, 2008.
- 15 Zheng, Z.-W. and Zheng, Q.: Variability of island-induced ocean vortex trains, in the Kuroshio region southeast of Taiwan Island, *Cont. Shelf Res.*, 81, 1–6, 2014.



(a)



(b)

Figure 1. (a) Schematic illustration of the study domain and the bathymetry derived from the ETOPO1 and (b) computational meshes with fine meshes used in the coastal waters around Lanyu Island and Green Island.

Typhoon effect on Kuroshio and Green Island wake: a modelling study

T.-W. Hsu et al.

Title Page	
Abstract	Introduction
Conclusions	References
Tables	Figures
◀	▶
◀	▶
Back	Close
Full Screen / Esc	
Printer-friendly Version	
Interactive Discussion	



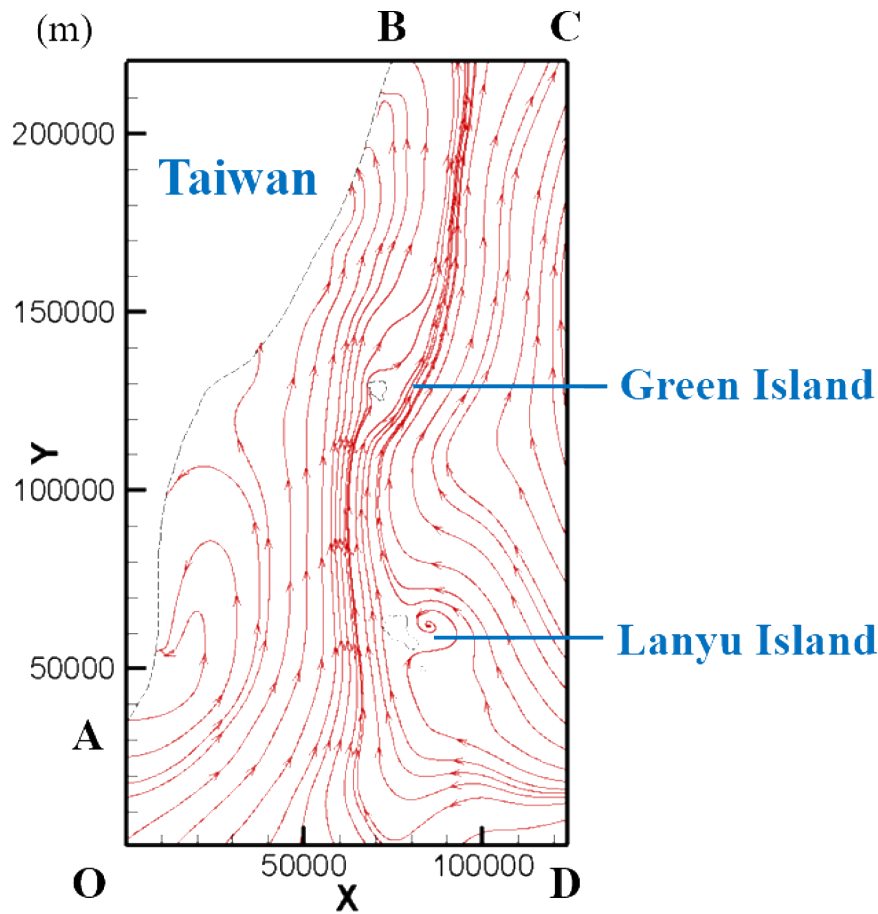


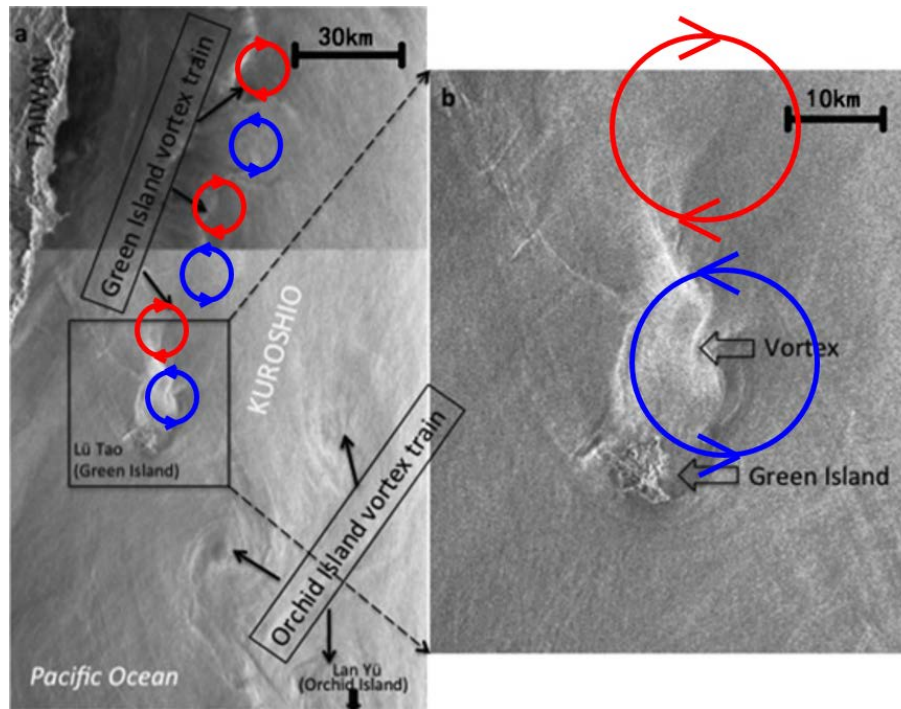
Figure 2. Study domain and boundaries as well as contours of flow speed from HYCOM.

Typhoon effect on Kuroshio and Green Island wake: a modelling study

T.-W. Hsu et al.

Title Page	
Abstract	Introduction
Conclusions	References
Tables	Figures
◀	▶
◀	▶
Back	Close
Full Screen / Esc	
Printer-friendly Version	
Interactive Discussion	





(a)

(b)

Figure 3. (a) A composite ERS-1 SAR image of island-induced ocean vortex trains of Lanyu Island and Green Island taken at 17:01 UT 25 September (lower) and 19:02 UT 2 October (top), 1996. (b) Zoomed Green Island and head of vortex train (modified from Fig. 2 of Zheng and Zheng, 2014).

Typhoon Soulik (7/7/2013 - 7/14/2013)

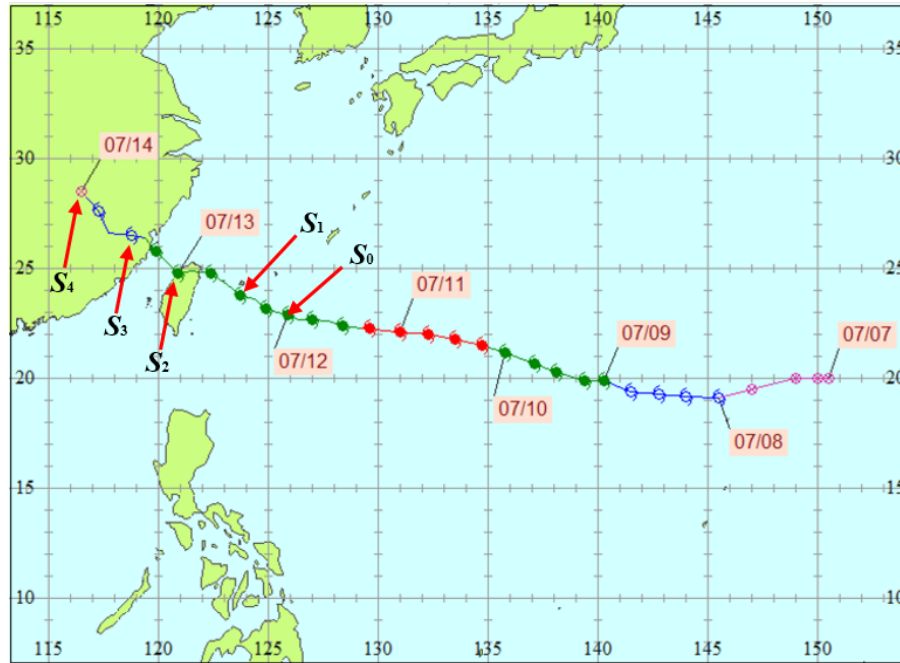


Figure 4. Track of typhoon Soulik from 7 to 14 July 2013, where symbol \otimes denotes the tropical depression with maximum wind speed $V_{\max} < 17.2 \text{ m s}^{-1}$; \circ the tropical storm, $17.2 < V_{\max} < 32.6 \text{ m s}^{-1}$; \bullet the moderate typhoon, $32.7 < V_{\max} < 50.9 \text{ m s}^{-1}$; \circ a severe typhoon, $51 \text{ m s}^{-1} < V_{\max}$, and S_0 – S_4 are the five time instances with a 12 h of increment to show the flow fields, see, for example, S_0 represents 00:00 of 12 July, S_1 12:00 of 12 July, S_2 00:00 of 13 July, S_3 12:00 of 13 July, and S_4 00:00 of 14 July 2013, respectively (modified from CWB of Taiwan).

Typhoon effect on Kuroshio and Green Island wake: a modelling study

T.-W. Hsu et al.

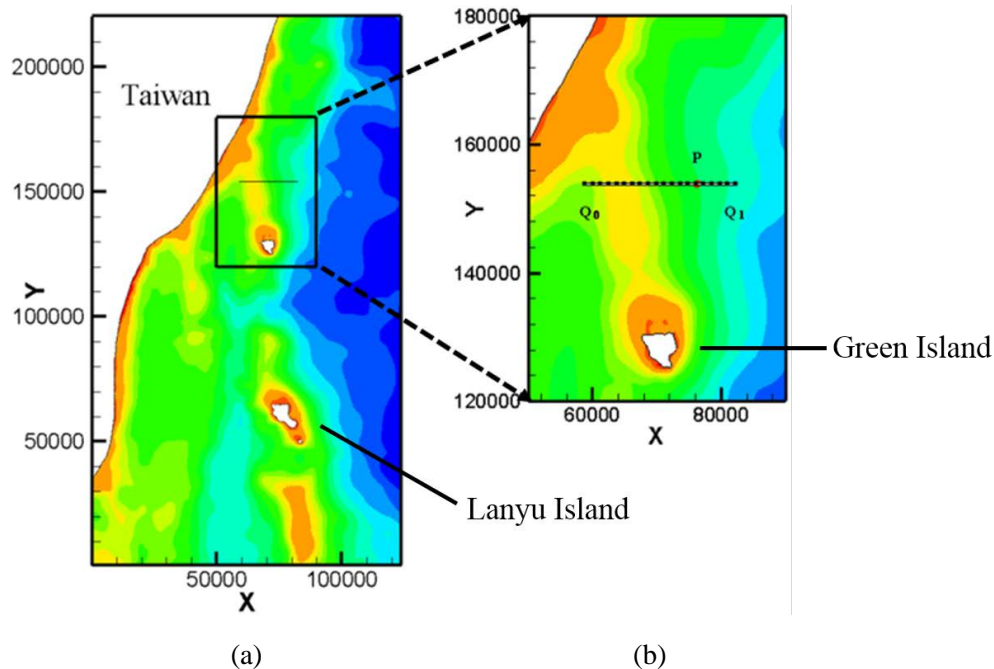


Figure 5. (a) Global view of the study area, where the enclosed region near the Green Island indicates the sub-domain that will be presented in the succeeding plots of the downstream recirculation and island wakes, and (b) local view of the sub-domain as well as location of the cross section Q_0Q_1 and monitor point P downstream Green Island. Length of Q_0Q_1 is 20 km. It locates about 22 km downstream the Green Island.

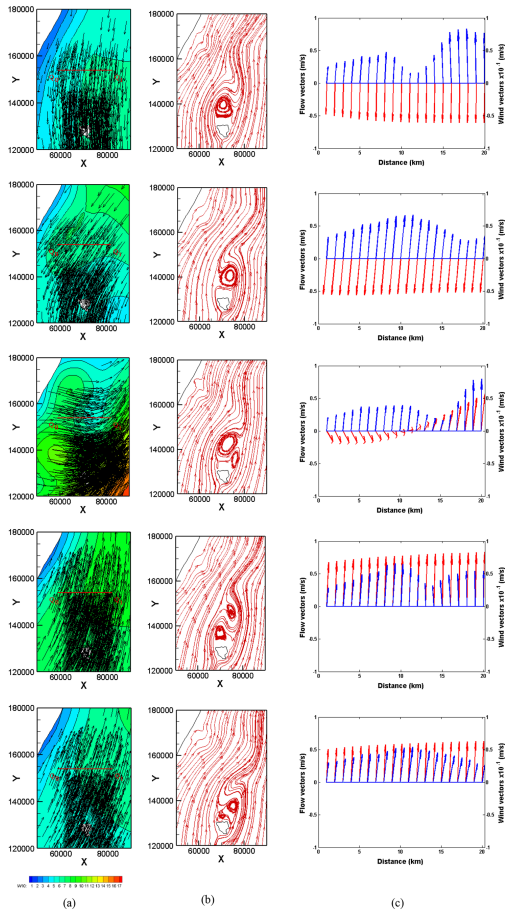


Figure 6. (a) W_{10} vectors and contours, (b) flow streamlines, and (c) wind vectors (red) and flow vectors (blue) of cross section $\overline{Q_0 Q_1}$ at S_0 – S_4 five time instances of the typhoon Soulik, see Fig. 5.

Typhoon effect on Kuroshio and Green Island wake: a modelling study

T.-W. Hsu et al.

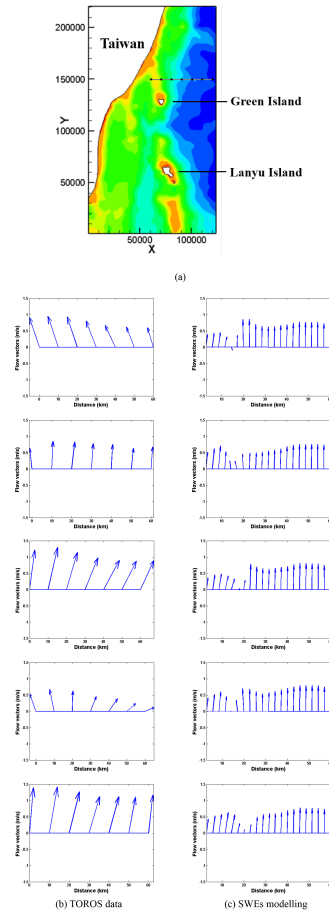


Figure 7. (a) Location of the 22.84° N ($y = 150$ km) cross section, where black dots denote the position of TOROS data. (b) and (c) depict comparison of flow vectors of TOROS data and model predictions along 22.84° N cross section at S_0 – S_4 five time instances, see Fig. 5.

Title Page

Abstract Introduction

Conclusions References

Tables Figures

◀ ▶

◀ ▶

Back Close

Full Screen / Esc

Printer-friendly Version

Interactive Discussion



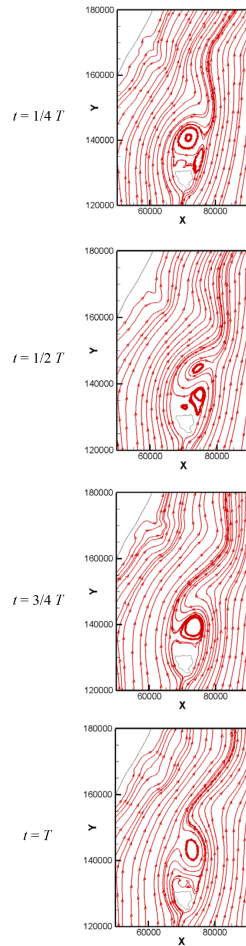


Figure 8. Flow streamlines of the Green Island wake of no wind forcing case.

Typhoon effect on Kuroshio and Green Island wake: a modelling study

T.-W. Hsu et al.

Title Page

Abstract Introduction

Conclusions References

Tables Figures

◀ ▶

◀ ▶

Back Close

Full Screen / Esc

Printer-friendly Version

Interactive Discussion



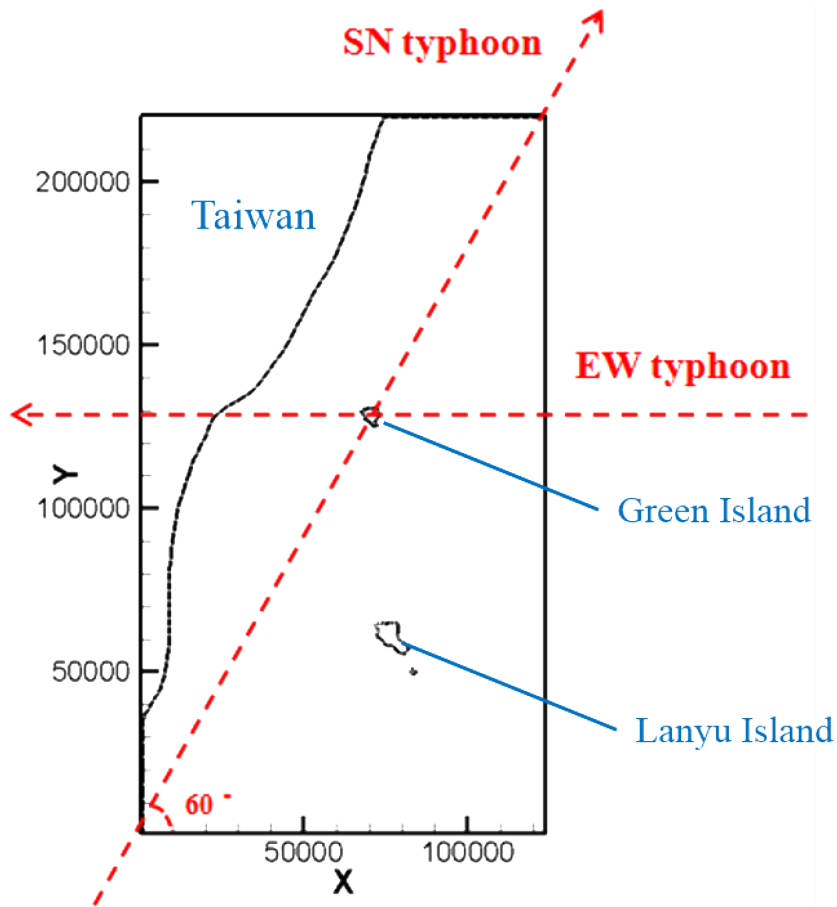


Figure 9. Schematic diagram of the study domain and track of SN and EW typhoon.

Typhoon effect on Kuroshio and Green Island wake: a modelling study

T.-W. Hsu et al.

Title Page	
Abstract	Introduction
Conclusions	References
Tables	Figures
◀	▶
◀	▶
Back	Close
Full Screen / Esc	
Printer-friendly Version	
Interactive Discussion	



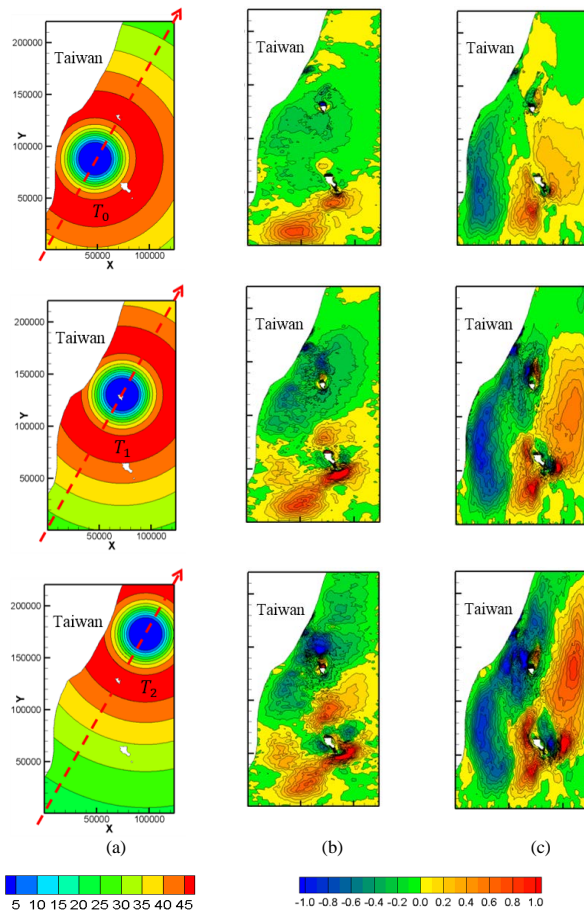


Figure 10. Contours of (a) W_{10} , “net” (b) u , and (c) v contours of SN typhoon with moving speed $W_T = 2.5 \text{ m s}^{-1}$ at T_0 – T_2 three time instances indicated by the three vertical lines of Fig. 16a.

Typhoon effect on Kuroshio and Green Island wake: a modelling study

T.-W. Hsu et al.

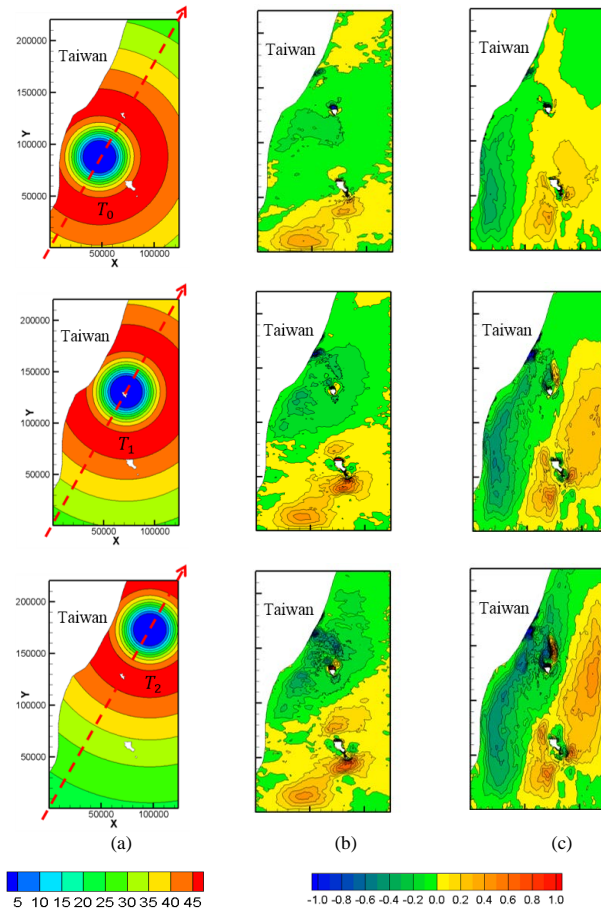


Figure 11. Contours of (a) $W_{10, \text{net}}$, (b) u , and (c) v contours of SN typhoon with moving speed $W_T = 5.0 \text{ m s}^{-1}$ at T_0 – T_2 three time instances indicated by the three vertical lines of Fig. 16b.

Title Page

Abstract Introduction

Conclusions References

Tables Figures

◀ ▶

◀ ▶

Back Close

Full Screen / Esc

Printer-friendly Version

Interactive Discussion



Typhoon effect on Kuroshio and Green Island wake: a modelling study

T.-W. Hsu et al.

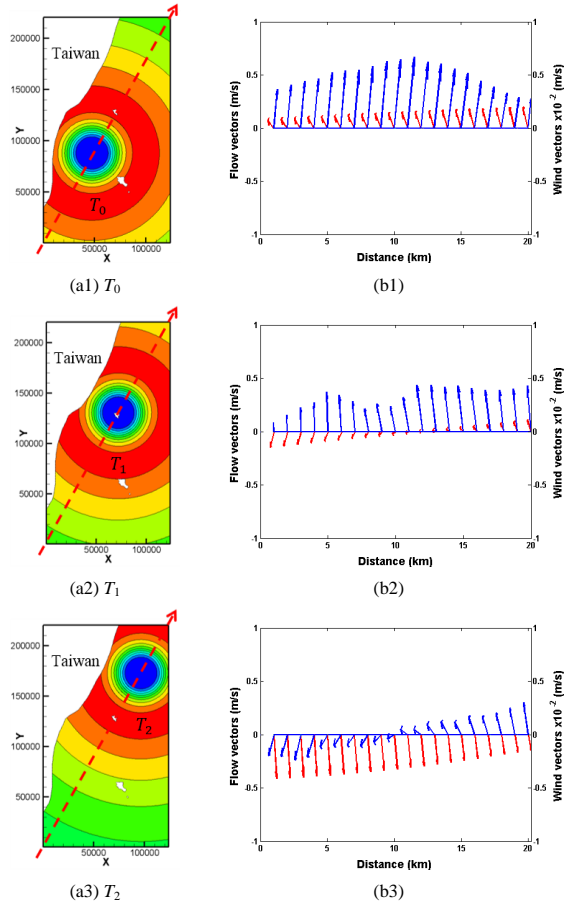


Figure 12. (a) W_{10} contours and **(b)** wind vectors (red) and flow vectors (blue) of SN typhoon along cross section $\overline{Q_0Q_1}$ with moving speed $W_T = 2.5 \text{ m s}^{-1}$ at T_0 – T_2 three time instances indicated by the three vertical lines of Fig. 16a.

Title Page

Abstract Introduction

Conclusions References

Tables Figures

◀ ▶

◀ ▶

Back Close

Full Screen / Esc

Printer-friendly Version

Interactive Discussion



Typhoon effect on Kuroshio and Green Island wake: a modelling study

T.-W. Hsu et al.

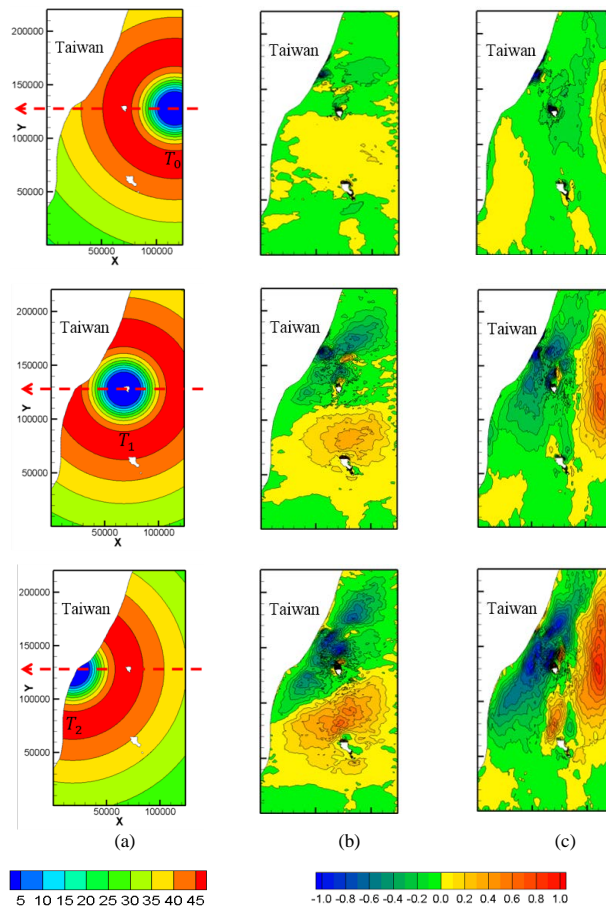


Figure 13. Contours of (a) W_{10} , “net” (b) u , and (c) v contours of EW typhoon with moving speed $W_T = 2.5 \text{ m s}^{-1}$ at three time instances T_0 – T_2 indicated by the three vertical lines of Fig. 16a.

Title Page

Abstract

Introduction

Conclusions

References

Tables

Figures

◀

▶

◀

▶

Back

Close

Full Screen / Esc

Printer-friendly Version

Interactive Discussion



Typhoon effect on Kuroshio and Green Island wake: a modelling study

T.-W. Hsu et al.

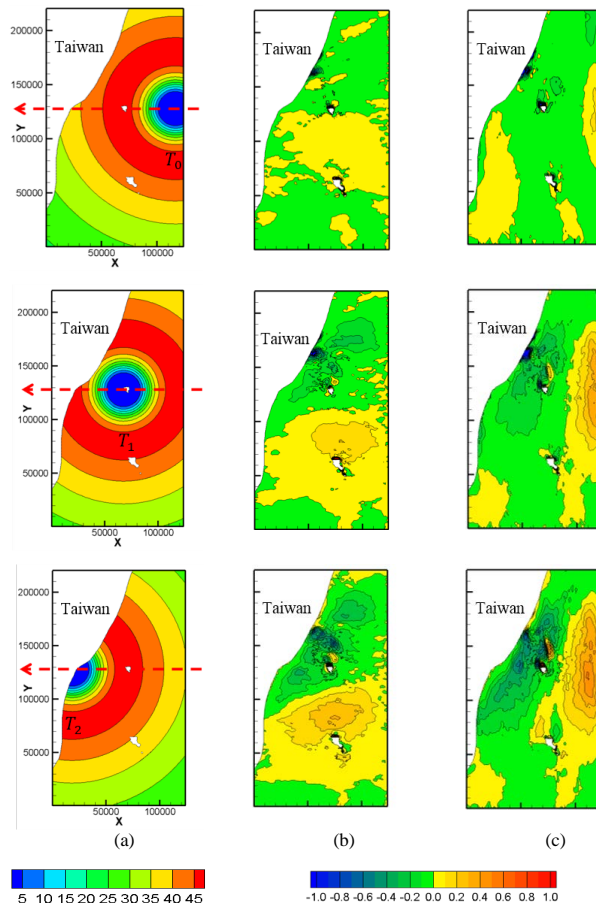


Figure 14. Contours of (a) W_{10} , “net” (b) u , and (c) v contours of EW typhoon with moving speed $W_T = 5.0 \text{ m s}^{-1}$ at T_0 – T_2 three time instances indicated by the three vertical lines of Fig. 16b.

Title Page

Abstract Introduction

Conclusions References

Tables Figures

◀ ▶

◀ ▶

Back Close

Full Screen / Esc

Printer-friendly Version

Interactive Discussion



Typhoon effect on Kuroshio and Green Island wake: a modelling study

T.-W. Hsu et al.

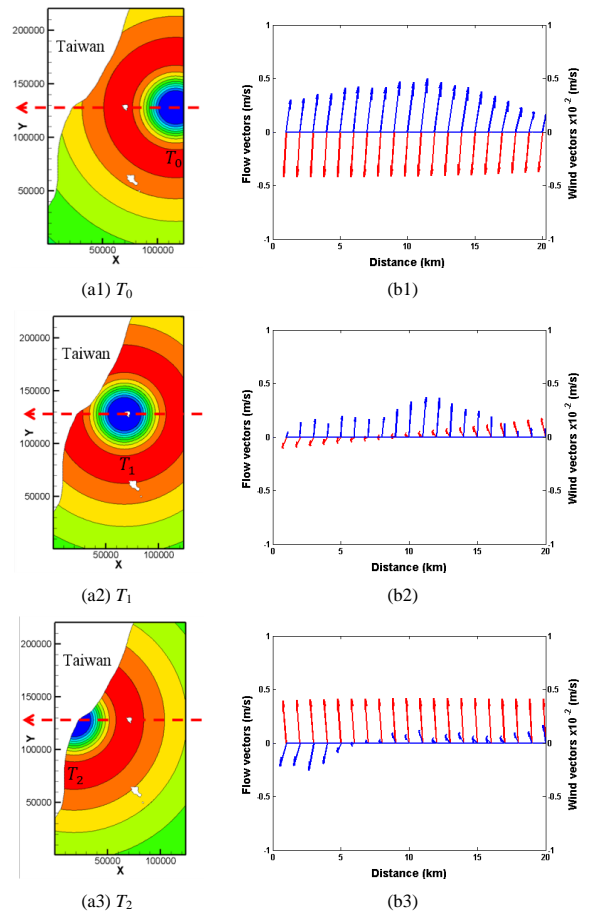


Figure 15. (a) W_{10} contours and (b) wind vectors (red) and flow vectors (blue) of EW typhoon along cross section $\overline{Q_0Q_1}$ with moving speed $W_T = 2.5 \text{ m s}^{-1}$ at T_0 – T_2 three time instances indicated by the three vertical lines of Fig. 16a.

Title Page

Abstract Introduction

Conclusions References

Tables Figures

◀ ▶

◀ ▶

Back Close

Full Screen / Esc

Printer-friendly Version

Interactive Discussion



Typhoon effect on Kuroshio and Green Island wake: a modelling study

T.-W. Hsu et al.

Title Page

Abstract

Introduction

Conclusions

References

Tables

Figures



Back

Close

Full Screen / Esc

Printer-friendly Version

Interactive Discussion

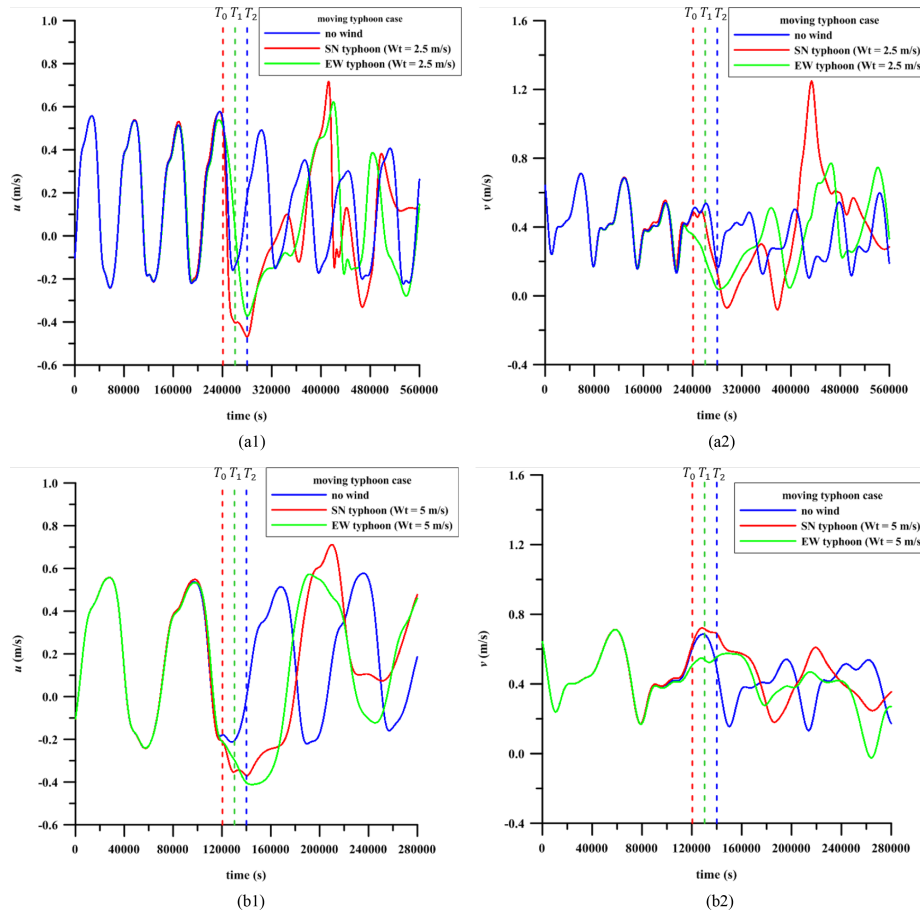


Figure 16. Comparison of u and v of monitor point P of no wind, SN, and EW typhoon with the moving speed $W_T =$ **(a)** 2.5 ms^{-1} (upper row) and **(b)** 5.0 ms^{-1} (lower row), respectively.